31st Annual International Conference of the IEEE EMBS
Minneapolis, Minnesota, USA, September 2-6, 2009

MRI Compatibility Evaluation of a Piezoelectric Actuator System for a Neural Interventional Robot

Yi Wang, Gregory A. Cole, Hao Su , Julie G. Pilitsis and Gregory S. Fischer

Abstract— **The work presented in this paper has been performed in furtherance of developing an MRI-compatible surgical robotic system, specifically targeting the neural intervention procedure for the treatment of Parkinson's Syndrome known as deep brain stimulation (DBS). In this paper we discuss the construction and testing of the MR-compatible controller, sensors and actuators, and the compatibility testing we have done to validate the success of our efforts in eliminating signal interference. Our robotic system was tested on a Phillips Achieva 3 Tesla MRI machine under diagnostic T1 and T2, high speed FGRE and functional EPI imaging protocols. It has been shown to operate without introducing any statistically significant degradation in image quality. We have shown that the creation of an MR-compatible electronically controlled closed-loop robotic actuation system and linkage mechanism can be created successfully within a standard high-field diagnostic magnet with insignificant levels of signal interference.**

I. INTRODUCTION

Deep brain stimulation (DBS) is a technique for influencing brain function though the use of precisely placed implanted electrodes for effective treatment of Parkinson's Disease and other movement disorders [1]. Studies show that DBS may be similarly effective in treating major depression and Alzheimer's Disease [2]. Successful outcomes require accurate localization of, and guidance of the electrode to, the target intra-operatively.

In typical DBS electrode insertion (Indirect MR guidance), preoperative MRI images of the brain's anatomy are acquired and used for planning. A fiducial frame is rigidly affixed to the patient who undergoes a CT scan just prior to surgery, where the images are spatially registered to the MR images. It is not typical to use further radiological guidance intraoperatively. Because of this, most centers have adopted electrophysiological confirmation (*i.e.* micro-electrode recordings (MER) to ensure proper intraoperative probe placement, though this step adds significantly to potential morbidity[3], and has a diminishing role in new applications/targets for DBS.

Direct MR guidance would streamline the procedure and allow for high precision image-guidance. However, the only MR-compatible stereotactic device for DBS reported to date is the Nexframe (Medtronic Minneapolis, MN). Studies with this device show a mean error of $1.0mm$ (range $0.1mm$ – $1.9mm$), which is comparable to indirect MR frame-based approaches; it is felt that the majority of this error was due to manual alignment of the cannula guide [4]. *Use of a robotic alignment guide would potentially eliminate this difficulty, improve work flow, and potentially improve the accuracy of the technique.*

A review of MR-compatible systems to date for image-guided interventions can be found in [5]. Robotic assistance has been investigated for guiding instrument placement in MRI beginning with neurosurgery [6]. Chinzei *et al* developed a general-purpose robotic assistant for open MRI based upon Shinsei ultrasonic motors[7]. An investigation into MR-compatibility of actuation techniques for functional imaging is reported in [8]. Suzuki *et al* describes ultrasonic motor drive techniques that enhance MR-compatibility in [9]. The feasibility of using piezoceramic motors for robotic prostate biopsy is described by Elhawary *et al* in [10].

While robotic guidance for MR-guided procedures has great value for this procedure, there currently does not exist a viable solution for MR-guided DBS lead placement. This paper reports the MR compatibility of a surgical robotic system currently being developed at Worcester Polytechnic Institute, as described by Cole *et al* [11] and shown in Fig. 1. The device is designed to mount beside the cranium, where it can rotate up to 60° in both the sagittal and transverse planes. At the end effector of the robot, there is a yolk which can provide two additional degrees of freedom (DOF) in the form of tilting the cannula guide to allow for any insertion angle at the targeted burr hole location. While the initial focus of our work is DBS, proving that the methods, materials and components used in this system are MR-compatible will provide building blocks for the design and construction of a

Fig. 1. The prototype robot in the bore of a 3T MRI scanner with the cannula targeting a model skull.

Yi Wang, Gregory A. Cole, Hao Su and Gregory S. Fischer are with the Department of Mechanical Engineering, Worcester Polytechnic Institute, Worcester, MA, USA gfischer@wpi.edu

Julie G. Pilitsis is with University of Massachusetts Medical School, Worcester, MA, USA

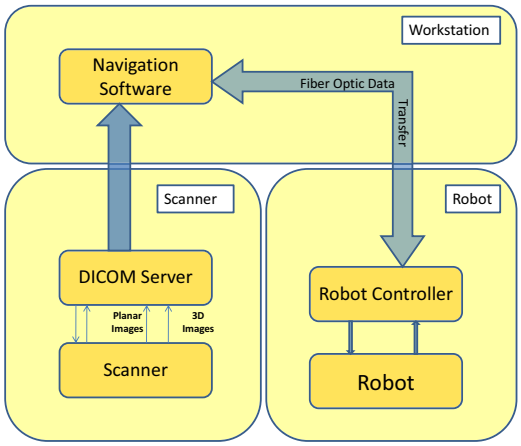

Fig. 2. Block diagram of the system architecture.

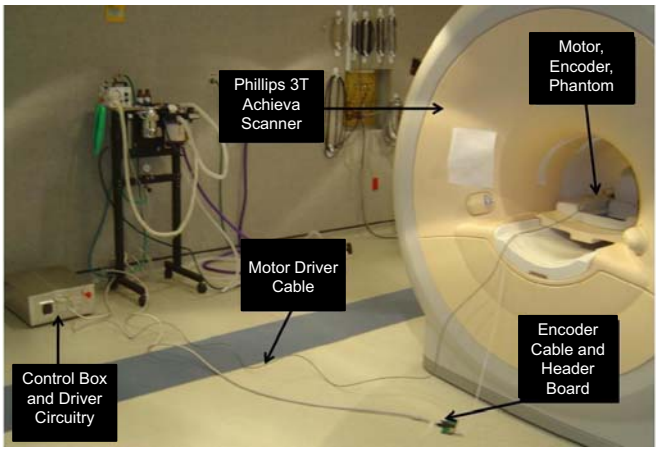

Fig. 3. Configuration of the robot controller with sensors and actuators active in the scanner during MR-compatibility experiments.

multitude of MR- compatible equipment in the future. The results demonstrate how the elements of a complete robotic system including a power supply, driver/controller, motor and encoder are able to be operate with little to no interference with the MRI Scanner.

II. System Overview

A. Prototype Construction

The first requirement of this system is that it should be MRI-compatible, which means that it is both MRI-safe and it will not produce noise and interference with the MRI scanner. The most difficult part of any MR-compatible mechatronic device is the sensors and actuators, as the nature of these devices operation generally causes interference with imaging quality. Although earlier experiments performed by Fischer and Krieger have shown piezoelectric motors to produce large amounts of interference with image quality while under motion when in their "off the shelf" configuration [12], we believe that this is primarily due to lack of shielding and filtering of the drive circuits; thus, we decided to produce our own motor driver boards and linear power supply in an attempt to reduce imaging interference.

The motor boards that were developed for this system, were made because available hardware to drive piezoelectric motors tends to be very expensive, and it is generally not possible to drive the motors with highly specific arbitrary waveforms. The Nanomotion single channel controller retails for close to $2,000 and offers no control over the shape of the drive waveform supplied and also employs a switching power supply which may negatively affect signal integrity. The piezo driver boards we are developing will fill the need for an MR-compatible motor driver with the option of generating a highly specific arbitrary waveform.

The overall system architecture of the device being studied is shown in Fig. 2, and is similar to that reported by Fischer *et al* for prostatic interventions [13]. Communication from the navigation software running on a laptop in the console room to the robot controller computer is through a fiber optic connection run through the patch panel, as this eliminates a large source of noise that is introduced when electrical signals are passed through the walls of the scanner room. In order to make the robotic device compatible, the armature mechanism itself has been constructed of high strength plastics such as Ultem and Peek. We have selected piezoelectric actuators due to the positive results for Nanomotion motors reported previously in a study by Fischer and Krieger *(*et al) [12]. However, we opted for the similar nonmagnetic versions of the Piezo LEGS (PiezoMotor, Uppsala, Sweden) ceramic actuators as described by Elhawary *et al* in [10] due primarily to the support available for custom motor controller design and availability of a compact rotary package. Our preliminary evaluation of an optimized version of the PiezoMotor actuators showed no more than 3% signal to noise ratio loss when operating in a 2T scanner [14]. We have created a custom control system for these motors that provides for low-cost, while being highly reconfigurable and ultra low noise for increased MR compatibility.

III. Materials and Methods

The experiments demonstrating MR-compatibility were performed in a Philips Achieva 3T system. The phantom employed in the experiment was a $12cm$ diameter plastic tube filled with a copper sulfate solution. It was placed of a $28cm$ diameter SENSE 8-element receive-only birdcage coil. The motor and encoder were placed immediately adjacent to the left side of the coil. The controller was placed approximately $3m$ from the scanner bore. No electrical connections pass out of the scanner room; power and ground to the linear power supply within the controller's chassis are provided through the in-room AC power source. The experimental configuration is shown in Fig.3.

Four imaging protocols were selected for evaluation of compatibility of the system: 1) diagnostic imaging T1-weighted fast gradient echo (T1 FGE/FFE), 2) diagnostic

TABLE I

SCAN PARAMETERS FOR COMPATIBILITY EVALUATION

Protocol	FOV	TE	TR	FA	Bandwidth
T1W FFE	240 mm	2.3 ms	225 ms	75^o	751 Hz/pixel
T2W TSE	240 mm	90 ms	3000 ms	90^o	158 Hz/pixel
FGRE	240 mm	2.1 ms	6.4 ms	50^o	217 Hz/pixel
SE EPI	240 mm	45 ms	188 ms	90^o	745 Hz/pixel

imaging T2-weighted fast spin echo (T2 FSE/TSE), 3) high-speed real-time imaging fast gradient echo (FGRE), and 4) functional imaging spin echo-planar imaging (SE EPI). Details of the scan protocol including field of view (FOV), echo time (TE), repetition time (TR), flip angle (FA), and bandwidth are shown in Table I; all sequences were acquired with a slice thickness of $5mm$ and a number of excitations (NEX) of one. Three configurations were evaluated and used in the comparison: 1) baseline of the phantom only, 2) motor and encoder unpowered with controllers DC power supply turned on, and 3) motor running at $12RPM$. Ten slices were acquired per imaging protocol for each configuration.

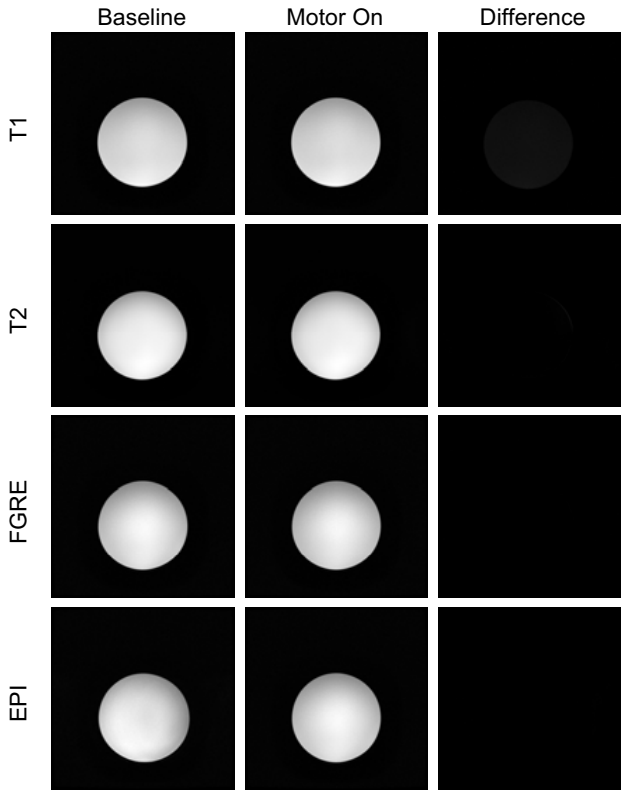

Fig. 4. Representative results showing the difference in images obtained of baseline and motor running conditions.

The signal to noise ratio (SNR) was utilized as the metric for evaluating MR-compatibility, based upon the NEMA standard definition for determining SNR [15]. SNR was calculated as the mean signal in the center of the phantom divided by the noise intensity outside the phantom. Mean signal is defined as the mean pixel intensity in the region of interest (ROI). The noise intensity is defined as the root

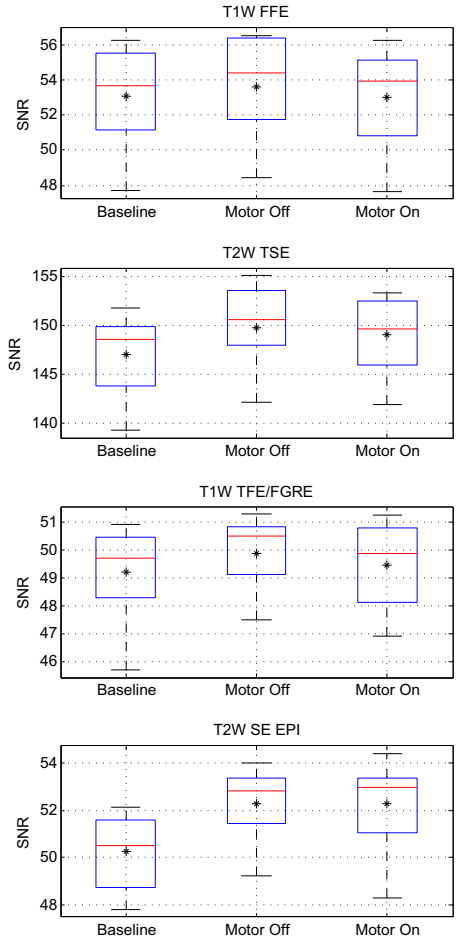

Fig. 5. Results of MR-compatibility analysis showing the SNR calculated from 10 images obtained for each sequence under each protocol and the plots represent the range of SNR.

mean square (RMS) signal intensity in an ROI outside of the phantom and not bordering on any artifacts or regions that are part of the phantom imaging.

IV. RESULTS

To determine the effectiveness of our efforts to minimize noise and interference with the scanner, first a subtraction noise analysis was performed. In this analysis, images obtained during motor operation in the scanner are subtracted from the baseline images; the new image visually depicts only the change in pixel values between the baseline and the test where the equipment is operating. As can be seen in Fig. 4, the motors and encoders provide almost no visually identifiable interference with the operation of the scanner, even while under motion.

The SNR for each of these imaging modalities under the Phillips 3T scanner is shown in Fig. 5. The boxplots show the variation in SNR for the 10 images taken in each configuration. The '*' represents the mean SNR, the horizontal line in the middle of the box represents the median, the top and bottom represent the quartiles, and the whiskers represent the

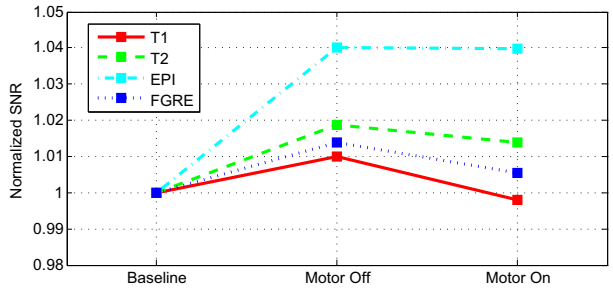

Fig. 6. Results of the normalized SNR under each protocol. No statistically significant variations exist between baseline and motor running conditions.

limits. Statistical analysis with a Tukey Multiple Comparison confirms that no pair shows a significant signal degradation with a 95% confidence interval. For comparison, the SNR for each configuration was normalized by the average SNR of the 10 baseline images for each imaging protocol. The result is shown in Fig. 6.

A. Discussion

This test has shown that if every component of a robotic control system is chosen carefully, and fully shielded an ultra low noise electric driven actuator system can be developed. Despite that the motors and encoders are operated relatively close to the scanner's imaging isocenter, the system still causes negligible interference with the scanner. Since we have already demonstrated the compatibility of the PC104-based control computer in our work on a robot for an MR-compatible robot for prostatic interventions [13], the success of the scanner tests described in this paper has shown that the sources of imaging interference produce an acceptably low contribution to SNR-variation of the imaging. We have successfully shown that a linear power supply and high speed and power arbitrary waveform amplifiers, as well as shielded cables we can safely generate precisely controlled motion inside a high field diagnostic scanner.

These are important results, because while we have shown that our robotic system will be MR-compatible once fully constructed and assembled. We have also shown that with a combination of mostly "off the shelf" products, an MR-compatible computer controlled system can be constructed and applied to any system architecture required. Due to the extremely low interference with the image quality shown in the test data, we expect that the scanner can be used to its full potential and produce high resolution and functional images for image-guided robot-assisted interventional procedures. Now that the compatibility of the electronics and actuation systems for the robot have been shown, we intend to complete the robotic device and begin system accuracy and workflow assessment.

V. Acknowledgements

This work is currently being funded by internal Worcester Polytechnic Institute funds. We would like to thank our collaborators at University of Massachusetts Memorial Hospital including Mitch Albert and Paul Dasari.

References

[1] G. Deuschl, et al., "A randomized trial of deep-brain stimulation for parkinson's disease.," *N Engl J Med*, vol. 355, pp. 896–908, Aug 2006.

[2] B. Aouizerate, et al., "Deep brain stimulation for ocd and major depression.," *Am J Psychiatry*, vol. 162, p. 2192, Nov 2005.

[3] P. A. Starr, C. W. Christine, P. V. Theodosopoulos, N. Lindsey, D. Byrd, A. Mosley, and W. J. Marks, "Implantation of deep brain stimulators into the subthalamic nucleus: technical approach and magnetic resonance imaging-verified lead locations.," *J Neurosurg*, vol. 97, pp. 370–387, Aug 2002.

[4] A. J. Martin, P. S. Larson, J. L. Ostrem, W. K. Sootsman, P. Talke, O. M. Weber, N. Levesque, J. Myers, and P. A. Starr, "Placement of deep brain stimulator electrodes using real-time high-field interventional magnetic resonance imaging.," *Magn Reson Med*, vol. 54, pp. 1107–1114, Nov 2005.

[5] N. V. Tsekos, A. Khanicheh, E. Christoforou, and C. Mavroidis, "Magnetic resonance-compatible robotic and mechatronics systems for image-guided interventions and rehabilitation: a review study.," *Annu Rev Biomed Eng*, vol. 9, pp. 351–387, 2007.

[6] K. Masamune, E. Kobayashi, Y. Masutani, M.Suzuki, T. Dohi, H. Iseki, and K. Takakura, "Development of an mri-compatible needle insertion manipulator for stereotactic neurosurgery.," *J Image Guid Surg*, vol. 1, no. 4, pp. 242–248, 1995.

[7] K. Chinzei, N. Hata, F. A. Jolesz, and R. Kikinis, "Mri compatible surgical assist robot: System integration and preliminary feasibility study," in *MICCAI*, vol. 1935, pp. 921–930, October 2000.

[8] R. Gassert, R. Moser, E. Burdet, and H. Bleuler, "Mri/fmri-compatible robotic system with force feedback for interaction with human motion," *IEEE Trans Mech*, vol. 11, pp. 216–224, April 2006.

[9] T. Suzuki, H. Liao, E. Kobayashi, and I. Sakuma, "Ultrasonic motor driving method for emi-free image in mr image-guided surgical robotic system," in *Proc. IEEE/RSJ International Conference on Intelligent Robots and Systems IROS 2007*, pp. 522–527, Oct. 29 2007–Nov. 2 2007.

[10] H. Elhawary, A. Zivanovic, M. Rea, B. Davies, C. Besant, D. McRobbie, N. de Souza, I. Young, and M. Lamprth, "The feasibility of mr-image guided prostate biopsy using piezoceramic motors inside or near to the magnet isocentre.," *Med Image Comput Comput Assist Interv Int Conf Med Image Comput Comput Assist Interv*, vol. 9, no. Pt 1, pp. 519–526, 2006.

[11] G. A. Cole, J. G. Pilitsis, and G. S. Fischer, "Design of a robotic system for mri-guided deep brain stimulation electrode placement," in *Proc. IEEE International Conference on Robotics and Automation ICRA 2009*, pp. 4450–4456, May 2009.

[12] G. S. Fischer, A. Krieger, I. I. Iordachita, C. Csoma, L. L. Whitcomb, and G. Fichtinger, "Mri compatibility of robot actuation techniques – a comparative study," *Int Conf Med Image Comput Comput Assist Interv*, Sept. 2008.

[13] G. S. Fischer, I. I. Iordachita, C. Csoma, J. Tokuda, S. P. DiMaio, C. M. Tempany, N. Hata, and G. Fichtinger, "Mri-compatible pneumatic robot for transperineal prostate needle placement," *IEEE/ASME Transactions on Mechatronics*, vol. 13, June 2008.

[14] Y. Wang, M. Shazeeb, C. Sotak, and G. S. Fischer, "Optimization of piezoelectric motors to enhance mr compatiblity for interventional devices," in *International Society for Magnetic Resonance in Medicine, 17th Scientific Meeting and Exhibition, Proceedings*, 2009.

[15] *Determination of Signal-to-Noise Ratio (SNR) in Diagnostic Magnetic Resonance Imaging, NEMA Standard Publication MS 1-2008*. The Association of Electrical and Medical Imaging Equipment Manufacturers, 2008.